Performance of DSSS Signal Transmission with SCM over Low-Frequency MMF Passbands

Jaruwat Patmanee and **Surachet Kanprachar**†, Non-members

ABSTRACT

The transmission of a high data rate signal over low-frequency passbands of multimode fibers is studied in this paper. The subcarrier multiplexing (SCM) technique is applied to mitigate the frequency-selective nature of the passbands, at which many nulls can degrade the signal transmission. The subcarrier frequencies must be chosen appropriately, especially for some low-frequency passbands; otherwise, poorly received subcarrier signals will be obtained, affecting the entire transmission. Rather than transmitting many subcarrier signals over these passbands, the direct sequence spread spectrum (DSSS) technique can be adopted. In this work, a high data rate signal is transmitted over 1 km of multimode fiber using the 3-dB modal band and six other low-frequency passbands. The signal is separated into four sub-signals transmitted over four different channels: the 3-dB modal band, two low-frequency passbands, and one passband (containing four low-frequency passbands). In the last passband, the sub-signal is transmitted using the DSSS, while the other sub-signals are transmitted through amplitude shift keying (ASK) modulation. The performance of the system is determined using the bit error rate (BER). The findings reveal that by applying the DSSS to some low-frequency passbands, robustness is obtained in the subcarrier frequency for use in the DSSS passband. A BER lower than 10^{-9} with a total data rate of 600 Mbps is achieved. This data rate is three times higher than the data rate obtained by the 3-dB modal band. This performance is achieved without applying any error-correction code.

Keywords: Bit Error Rate, BER, Direct Sequence Spread Spectrum, DSSS, Multimode Fibers, 4-Amplitude Shift Keying, 4-ASK, Subcarrier Multiplexing

1. INTRODUCTION

Optical communication systems using multimode fiber are widely used for short-haul communication systems, such as those located indoors and between buildings. However, the most commonly used multimode fiber bandwidth, the 3-dB modal, is limited to 200 to 500 MHz·km. This limitation depends on the characteristics of the fiber, such as the type and length. A frequency region higher than the 3-dB modal band of the MMF has previously been utilized [1–4] to overcome the bandwidth limitation along with the low-frequency region of MMF. For an MMF of 1 km, a low frequency ranging from 0.2 to 1.6 GHz, which is next to the 3-dB modal band, has also been studied [5]. At this frequency range, the MMF frequency response is found to be frequency-selective, meaning that some passbands and nulls are available in the response. Signal degradation can certainly be introduced when sending a signal over this frequency range if some are located at the nulls. The center of these passbands can be estimated [5] and used to transmit a signal using subcarrier multiplexing (SCM) [6, 7].

To increase the data rate of the signal, 4-Amplitude shift keying (4-ASK) has previously been applied to the subcarrier signal transmitted over the 3-dB modal band [8]. A 500 Mbps signal has been transmitted over the 3-dB modal band and some low-frequency passbands of MMF with a bit error rate (BER) of lower than 10^{-9}. It should be noted that some passbands have not been used due to their unreliable nature. To lessen the effect of frequency-selective channels, the direct sequence spread spectrum (DSSS) has been shown to be a potential approach [9–14]. In the DSSS, an original signal is multiplied by a known signal to spread the bandwidth of the original signal, increasing the tolerance to the frequency-selective effect. Hence, in this work, the DSSS is adopted to utilize unreliable low-frequency passbands. A high data rate signal is transmitted over MMFs using SCM. One subcarrier signal is transmitted over different numbers of consecutive low-frequency passbands. The rest subcarrier signals are transmitted over the 3-dB modal band and other low-frequency passbands. The performance in terms of the total data rate and obtained BER are examined in this study. The robustness of the center frequency for use in the DSSS subcarrier signal is also provided.

The remainder of this paper is organized as follows. Section 2 describes the related theory. In Section 3, the multimode communication system model and BER determination are explained. Section 4 presents and discusses the simulation results, while Section 5 summarizes the work.

Manuscript received on September 27, 2021; revised on November 25, 2021; accepted on December 22, 2021. This paper was recommended by Associate Editor Piya Kovintavewat.

The authors are with the Department of Electrical and Computer Engineering, Naresuan University, Phitsanulok, Thailand.

†Corresponding author: surachetka@nu.ac.th

Digital Object Identifier: 10.37936/ecti-eec.2022202.246907

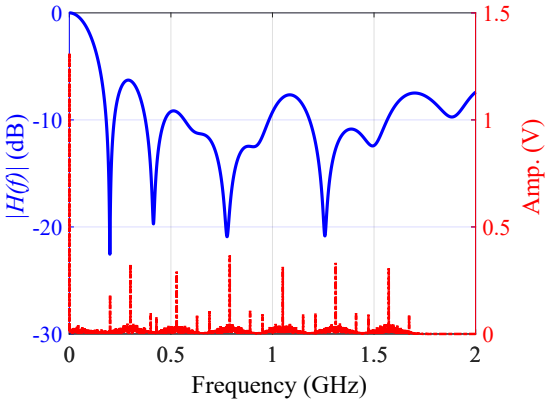

***Fig. 1**: The magnitude response of an MMF and the subcarrier signals in the frequency domain [7].*

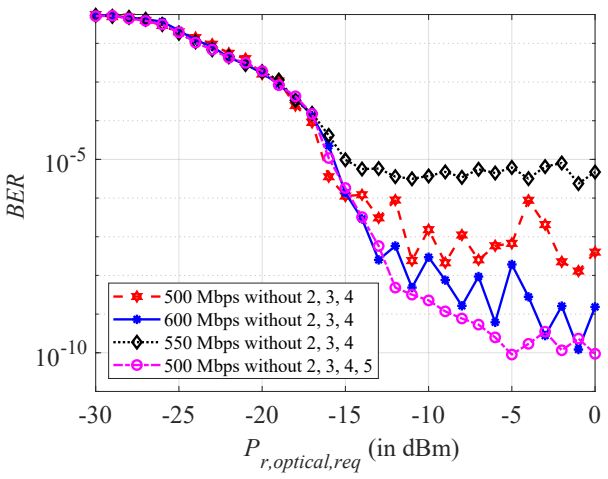

***Fig. 2**: Average BERs from 10 different MMFs [8].*

2. RELATED THEORY

2.1 Low-Frequency MMF Passbands

The frequency response of MMFs [5] can be determined, as shown in Eq. (1).

$$H_{fiber}(f) = \sum_{n=1}^{N_{mode}} e^{-j2\pi f t_{d,n}} \tag{1}$$

where $H_{fiber}(f)$ is the frequency response of the MMF, N_{mode} is the number of guided modes, and $t_{d,n}$ is the delay time of the n^{th} mode, which can be modeled as a uniform random variable.

As can be observed, the MMF frequency response depends on the delay times of its guided modes. The different delay times are due to the various guided modes traveling on different paths. Thus, the time required to reach the other end of the fiber differs. This then leads to a time spread of the received signal, namely multimode dispersion. The delay times in Eq. (1) can be defined statistically as a uniform random variable with an average time delay of $t_{d,avg}$ and a standard deviation of $t_{d,dev}$. The probability density function of the delay times ($t_{d,n}$) is given in Eq. (2).

$$f_{t_{d,n}}(t_{d,n}) = \begin{cases} \dfrac{1}{2t_{d,dev}}; & t_{d,avg} - t_{d,dev} \le t_{d,n} \le t_{d,avg} + t_{d,dev} \\ 0; & \text{otherwise.} \end{cases} \tag{2}$$

The frequency response of MMFs in the low-frequency region has recently been studied [5, 6], with many passbands available at low frequencies, ranging from 0.2–1.6 GHz. These passbands can be used as channels to send many signals. In previous analysis [5], at a frequency of between 0 and 1.6 GHz, seven possible channels were identified, including the 3-dB modal band and six other low-frequency passbands. The optimum peak frequencies used as subcarrier frequencies for these channels have been identified [6], namely 0, 300, 528, 789, 1050, 1311, and 1572 MHz, respectively. These passbands have been used as channels for sending a high data rate signal [7], as shown in Fig. 1.

Fig. 1 shows the magnitude response of an MMF and the seven subcarrier signals in the frequency domain. The peak frequency of the subcarrier signal from passband #3 (at 789 MHz) is located at the null of the response, resulting in a poor signal being received and a high BER from passband #3. This clearly suggests that passband #3 should not be used as a channel. Furthermore, the findings of the study reveal that the use of frequencies 528 and 1050 MHz for passbands #2 and #4 is not reliable since they are located at the nulls (or in the vicinity of the nulls) of other fibers. Thus, passbands #2 and #4 should not be utilized as channels either. Consequently, only four passbands are available: passbands #0 (the 3-dB modal band), #1, #5, and #6. The performance in terms of BER for the optical communication system using these four passbands has previously been studied [8], as shown in Fig. 2.

Fig. 2 shows four different BER curves from various total data rates and passbands. Each BER curve represents the averaged BER from 10 different MMFs. As can be observed, with a data rate of 600 Mbps (shown by the solid blue line with asterisk markers), when the received optical power ($P_{r,optical,req}$) is higher than −4 dBm, BER curves less than 10^{-8} are obtained. Four passbands are used: #0, #1, #5, and #6. Reducing the data rate transmitted over passband #5 in the hope of obtaining less BER than 10^{-8} appears to be ineffective, as indicated by the BER curve with the dotted black line and diamond markers. It can therefore be concluded that the use of passband #5 in subcarrier multiplexing transmission is not recommended. This is clearly demonstrated by the lowest BER curve (shown by a dash-dotted pink line with circle markers). In this case, only passbands #0, #1, and #6 are utilized, resulting in a total data rate of 500 Mbps with a BER of less than 10^{-9}.

As can be observed from the results, the signal received from passband #5 is also degraded from the null of fiber response. However, the attenuation in this

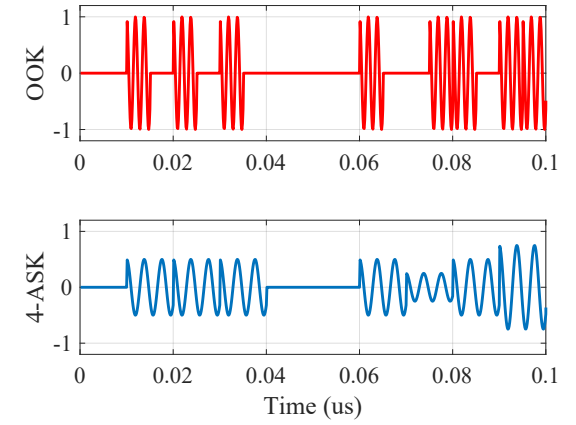

(a) Time domain

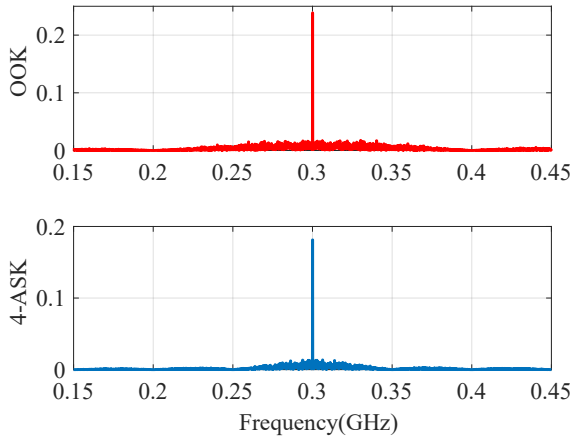

(b) Frequency domain

***Fig. 3**: OOK and 4-ASK in time and frequency domains.*

passband is lower than that of passbands #2, #3, and #4. According to previous research [7, 8] a very high attenuation from fiber response almost occurs in passbands #2, #3, and #4. To mitigate the frequency-selective fading channel problem in passbands #2, #3, and #4, the DSSS is adopted in this study. Passbands #2, #3, and #4 are combined into one, called the DSSS passband. Therefore, the five passbands used in this study are #0, #1, DSSS, #5, and #6. The corresponding fpeak,avg for these five passbands are 0, 300, 800, 1311, and 1572 MHz, respectively.

2.2 4-Amplitude Shift Keying (4-ASK)

Based on the amplitude shift keying (ASK) [15], 4-amplitude shift keying (4-ASK) is a type of digital modulation. In ASK, the modulating signal only changes the amplitude of the carrier signal, as shown in Eq. (3).

$$s_{ASK}(t) = A_c m(t) \cos(\omega_c t) \tag{3}$$

where A_c is the amplitude of the carrier signal, $m(t)$ is the modulating signal, and ω_c is the carrier frequency.

In the binary case, there are two possible values of the $m(t)$ to represent bits 0 and 1. If bit 0 is represented

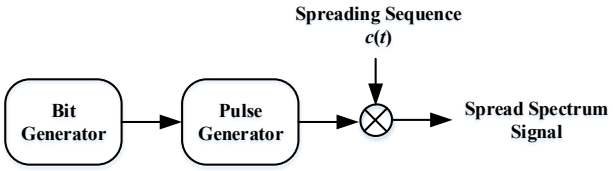

(a) Transmitter

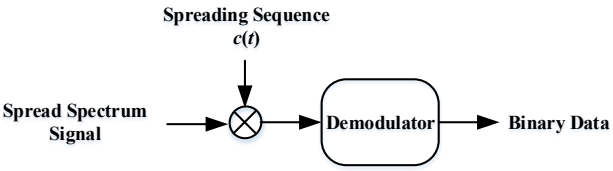

(b) Receiver

***Fig. 4**: Direct sequence spread spectrum (DSSS) model.*

by amplitude 0 and bit 1 by amplitude 1, ASK will be referred to as on-off keying (OOK). As can be observed, with two possible levels of $m(t)$, each signal in Eq. (3) can represent only 1 bit. On the other hand, in 4-ASK, there are four possible levels of $m(t)$; thus, four different signals in Eq. (3) are obtained. Each possible signal then represents two bits: 00, 01, 10, or 11. Examples of the signals transmitted using OOK and 4-ASK in time and frequency domains are shown in Fig. 3.

Fig. 3(a) shows the OOK and 4-ASK signals in the time domain. The data rate for transmitting these signals is set at 100 Mbps. It can be observed that the OOK signal has only two amplitudes: 0 and 1, meaning that only one information bit can be transmitted over one OOK signal. On the other hand, the 4-ASK signal has four amplitudes: 0, 0.25, 0.5, and 0.75. This means that for any 4-ASK signal, two possible bits can be transmitted. The frequency representation of these signals is shown in Fig. 3(b). As can be clearly observed, considering the null-to-null bandwidth, the required transmission bandwidth for 4-ASK is only half that required by OOK. This means that if the proposed channel is stable in terms of frequency response, the data rate to be transmitted over this channel can be increased two-fold with 4-ASK modulation rather than OOK. In this study, 4-ASK modulation is adopted for passband #0 and OOK for passbands #1, DSSS, #5, and #6, respectively.

2.3 Direct Sequence Spread Spectrum (DSSS)

The DSSS increases the tolerance for signal transmission over a frequency-selective fading channel. This technique reduces the probability of interception. The DSSS [16, 17] is one of two main spread spectrum techniques, the other being the frequency hopping spread spectrum (FHSS), which adopts a different approach but retains the same idea in terms of utilizing a larger channel bandwidth. The DSSS system model is shown in Fig. 4.

The DSSS transmitter diagram is shown in Fig. 4(a). The data bit stream is created at the bit generator. The generated bits are then fed into the pulse generator,

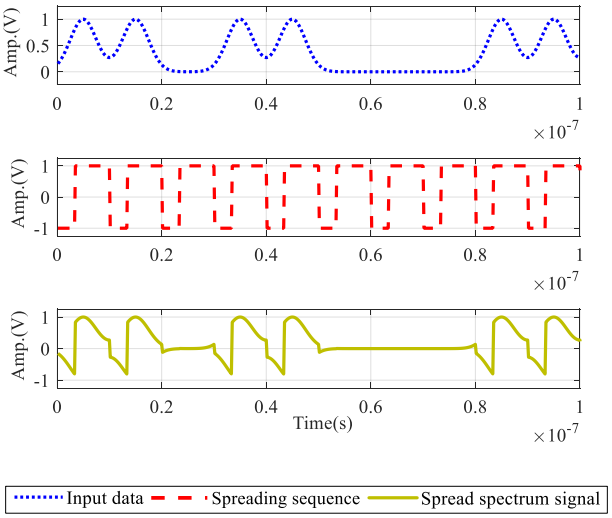

(a) Time domain

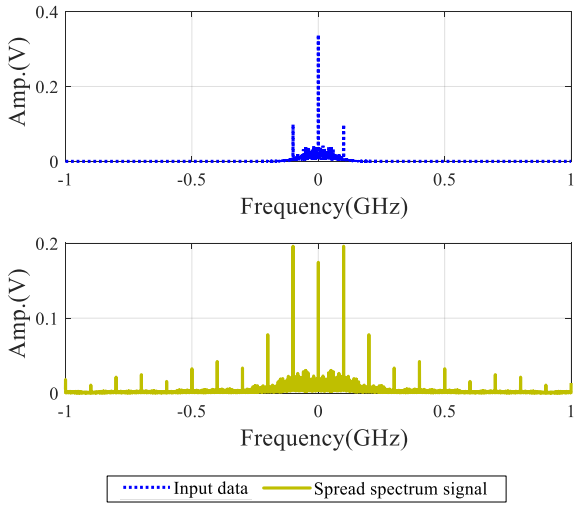

(b) Frequency domain

***Fig. 5**: Examples of signals in the direct sequence spread spectrum (DSSS).*

where the original signal is produced. This original signal is multiplied by a series of digits known as a spreading sequence ($c(t)$). The duration of each digit in the spreading sequence is smaller than the bit period of the original signal. After multiplication, the bandwidth of the resulting signal is increased or spread out and then called the spread spectrum signal. The receiving part of the DSSS is shown in Fig. 4(b). The received spread spectrum signal is multiplied by the same spreading sequence to demodulate the received spread spectrum signal back to the original signal without spreading out the bandwidth. Finally, the signal is fed into the demodulator to recover the original data. Examples of signal transmission using DSSS in the time and frequency domains are shown in Fig. 5.

The time domain signals in the DSSS transmission are given in Fig. 5(a). The upper plot shows the original input signal. As can be observed in this plot, the bit period

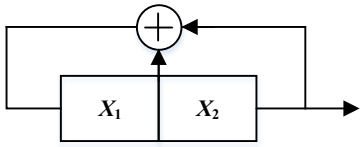

***Fig. 6**: Binary shift register with a feedback model for the irreducible polynomial of $x^2 + x + 1$.*

***Table 1**: Spreading sequence generated from the irreducible polynomial of $x^2 + x + 1$.*

X_1	X_2	Output
1	0	0
1	1	1
0	1	1

of the original signal is 0.1 μs, or the input signal data 10 Mbps. The spreading sequence is shown in the middle plot of Fig. 5(a). The sequence contains rectangular pulses called chips. Each chip has a smaller period compared to the bit period of the original signal. The chips are in a pseudorandom sequence of +1 and −1, with a repetition period equal to that of the input signal. After multiplying the original signal with the spreading sequence, the spread spectrum signal is obtained, as indicated in the lower plot of Fig. 5(a). Frequency representations of the original and spread spectrum signals are shown in Fig. 5(b). As can be clearly observed, after multiplying the spreading sequence to the original signal, the frequency components of the signal are spread out, covering a larger bandwidth, while the amplitude of these components is reduced to maintain the identical power of the original signal.

One possible way to create the spreading sequence is to use a binary shift register with feedback. The generated spreading sequence is called the maximal-length sequence or m-sequence. An example of a binary shift register with feedback is shown in Fig. 6.

This type of spreading code is based on the irreducible polynomials in Galois field theory. The order m of the irreducible polynomial determines the number of shift registers used in the model. As presented in Fig. 6, the shift register model is constructed according to the irreducible polynomial $x^2 + x + 1$, the order of which is 2 [18]. Applying the initial states of these two shift registers as 1 and 0 to the model shown in Fig. 6, the resulting output for the first chip period is then 0, and the states for the two shift registers are changed to 1 and 1. The process is repeated after running for three chip periods, as shown in Table 1. As can be observed, the output spreading sequence of 0, 1, 1, obtained from the last column in Table 1 is generated repeatedly. The codelength of the sequence is 3. It should be noted that the chip period is one-third of the original signal period. Multiplying this spreading sequence to the original signal, the bandwidth of the resulting spread

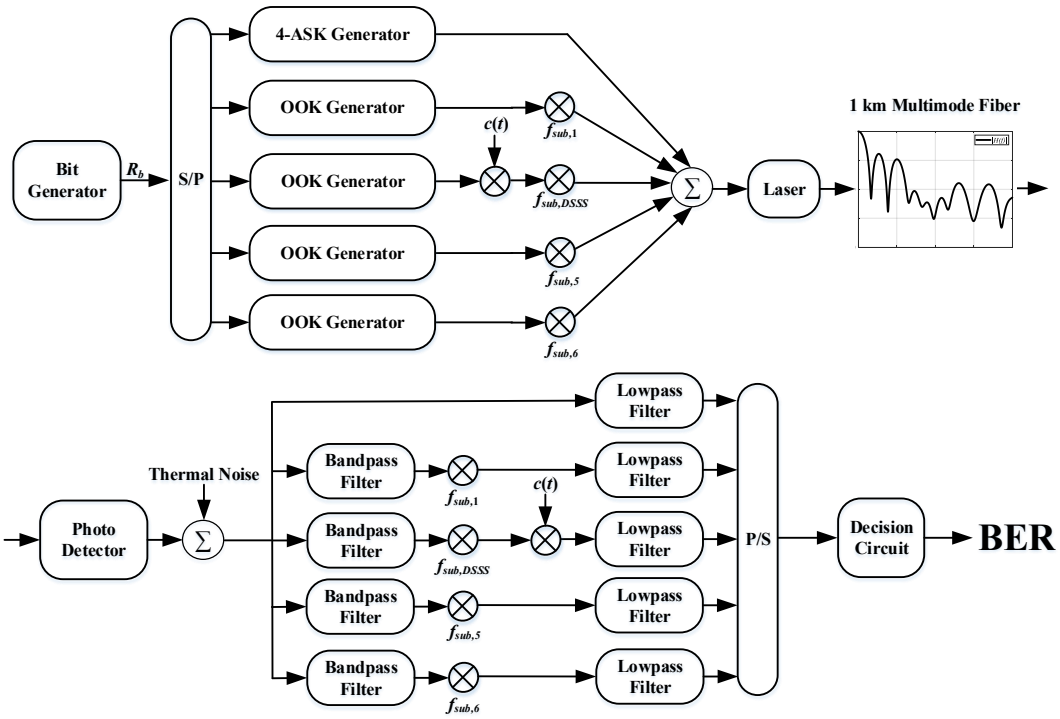

***Fig. 7**: MMF communication model using SCM and DSSS.*

signal is three times greater than the original signal, as shown in Fig. 5(b). In this study, this spreading sequence with a code length of 3 is adopted for use with the DSSS passband. Additionally, the center subcarrier frequency for carrying this DSSS signal will be varied to determine the robustness of the communication system under consideration.

3. METHODOLOGY

3.1 Optical Communication System

In this section, the model of the MMF communication system with SCM and DSSS is shown in Fig. 7.

In Fig. 7, the input data bits are generated by the bit generator block with a data rate of R_b. These data bits are sent to a serial-to-parallel (S/P) block for division into five different paths. For the first path, the divided data bits are sent to the 4-ASK generator to create a 4-ASK signal. For the other four paths, each of the divided data bits is sent to an OOK generator to create four OOK signals with different subcarrier frequencies: $f_{sub,1}$, $f_{sub,DSSS}$, $f_{sub,5}$, and $f_{sub,6}$, respectively. The corresponding frequencies for $f_{sub,1}$, $f_{sub,DSSS}$, $f_{sub,5}$, and $f_{sub,6}$ are 0, 300, 800, 1311, and 1572 MHz, respectively. As mentioned in Section 2, for the third path, an OOK signal is multiplied by the spreading sequence ($c(t)$) with a code length of 3 to create a spread signal. All five subcarrier signals are then combined and sent to a laser for signal transformation from an electric signal into a light signal. An MMF measuring 1 km is used to transmit the light signal, with $t_{d,avg} = 5\,\mu$s, $t_{d,dev} = 2.5$ ns, $N_{mode} = 100$ modes. At the signal destination, the received light signal is detected by a p-i-n photodetector and converted back into the received electrical signal. Thermal noise is added to the signal. The received electrical signal is then sent to five different paths according to five different subcarrier frequencies. For the third path, the received electrical signal is multiplied by the same spreading code ($c(t)$) to obtain the original signal. Each demodulated signal is sent to a decision circuit to estimate the received output bits, which are combined at the parallel-to-serial (P/S) block. The performance of this MMF communication system is measured by the BER for different transmission settings.

3.2 Bit Error Rate (BER)

The effectiveness of digital communication systems can be measured by the bit error rate variable (BER). BER is described by the probability of interpreting any received bit incorrectly. Normally, the minimum required BER for the optical communication system is lower than 10^{-9}. The OOK signal transmission referred to in Section 2.1 has two different levels for representing bits 0 and 1. Hence, at the receiving end, the BER in this case [19] can be calculated from the average of the received signal for bits 0 and 1 (that is, μ_0 and μ_1) and the standard deviations of the received signal for bits 0 and 1 (that is, σ_0 and σ_1), as shown in Fig. 8(a).

With the average amplitudes and standard deviations of bits 1 and 0, the BER for this OOK transmission is as follows:

$$BER_{OOK} = K\left(\frac{\mu_1 - \mu_0}{\sigma_1 + \sigma_0}\right) = K(x) \tag{4}$$

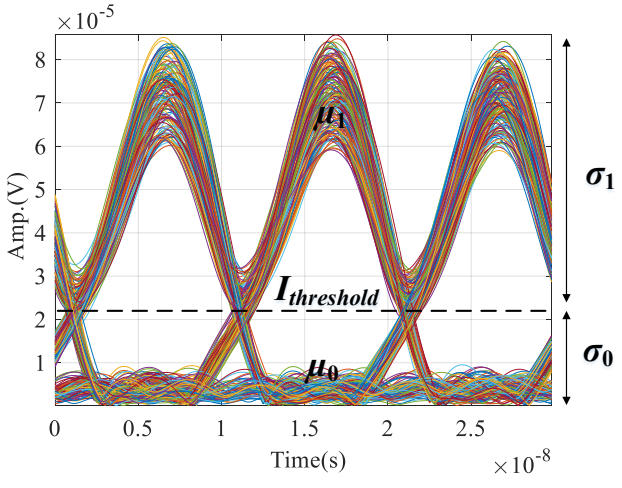

(a) OOK signal

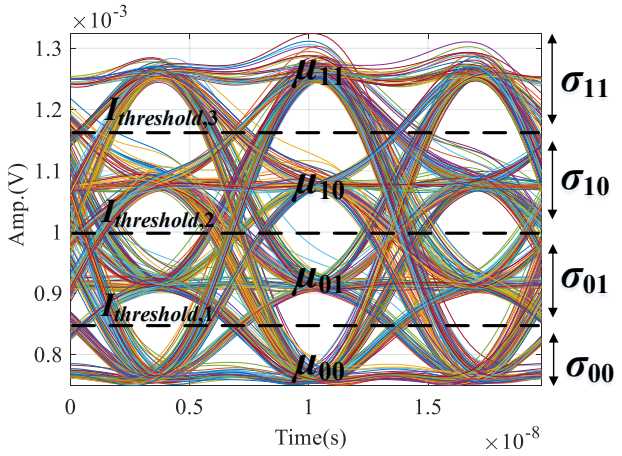

(b) 4-ASK signal

***Fig. 8**: Eye pattern from the received signal.*

where μ_0 and μ_1 are the average amplitude of the received signal for bits 0 and 1, respectively. σ_0 and σ_1 are the standard deviation of the received signal for bits 0 and 1, respectively. K is the probability that a zero-mean unit-variance Gaussian random variable exceeds x.

In the case of 4-ASK signal transmission, there are four different levels. Each level represents two bits, namely 00, 01, 10, and 11. Thus, at the receiving end, the BER in this case [20] can also be determined from the average of the received signal for bits 00, 01, 10, and 11 (that is, μ_{00}, μ_{01}, μ_{10}, and μ_{11}, respectively) and the standard deviations of the received signal for bits 00, 01, 10, and 11 (that is, σ_{00}, σ_{01}, σ_{10}, and σ_{11}, respectively), as shown in Fig. 8(b). The BER, in this case, is then determined as follows.

$$BER_{4-ASK} = \frac{1}{4}\left[K\left(\frac{\mu_{01}-\mu_{00}}{\sigma_{01}+\sigma_{00}}\right) + K\left(\frac{\mu_{10}-\mu_{01}}{\sigma_{10}+\sigma_{01}}\right) + K\left(\frac{\mu_{11}-\mu_{10}}{\sigma_{11}+\sigma_{10}}\right)\right] \quad (5)$$

In this work, 4-ASK modulation is applied to the signal transmitted over passband #0 and OOK modulation to the signals transmitted over passbands #1, DSSS, #5, and #6. Hence, five subcarrier signals (including that of passband #0) are used in this study. Applying Eqs. (4) and (5) to the subcarrier signals, the BER system can be determined as follows:

$$BER = \sum_{i=0}^{4} w_i BER_{SCM,i} \quad (6)$$

where w_i is the weighting factor defined from the ratio between the data rate sent by the i^{th}-subcarrier signal and the total system data rate and $BER_{SCM,i}$ is the BER of the i^{th}-subcarrier signal.

4. RESULTS AND DISCUSSION

In this section, the performance of the subcarrier multiplexing system transmitting signals over 1 km MMFs is studied. Ten different MMFs are used with $N_{mode} = 100$, $t_{d,avg} = 5\,\mu$s, and $t_{d,dev} = 2.5$ ns. These parameters are applied to Eqs. (1) and (2) to generate different MMF frequency responses. The MMF frequency responses will be different since the delay times shown in Eq. (2) are randomly selected according to the uniform distribution and given parameters, allowing the general performance of the proposed technique to be observed.

4.1 Maximum Data Rate for the 3-dB Modal Band

According to [5], the bandwidth of the 3-dB modal band (or passband #0) of MMFs measuring 1 km in length is approximately 200 MHz. Applying an OOK signal with different data rates, R_b, (that is, 150, 175, 200, and 225 Mbps, respectively) to the 3-dB modal band, the BERs obtained from the 10 different MMFs are presented in Fig. 9.

Fig. 9 shows the BERs from 10 different MMFs. Different data rates are used to determine the limit of the maximum data rate to be transmitted. Figs. 9(a) to 9(d) indicate that as the received optical power ($P_{r,optical,req}$) increases, the BERs from all 10 MMFs decrease monotonically. However, according to the data rate of 225 Mbps in Fig. 9(d), there is a case in Fiber 10 when the obtained BER does not monotonically decrease but becomes relatively flat at a BER of 10^{-4}. This means that the 225-Mbps signal is not guaranteed to be successfully transmitted over the 3-dB modal band of the MMFs. A maximum data rate of 200 Mbps can be transmitted over the 3-dB modal band with OOK modulation.

To increase the data rate of signal transmission over passband #0, the 4-ASK signal is applied with data rates of 300, 350, 400, and 450 Mbps. The obtained BERs from 10 different MMFs are shown in Fig. 10.

The BERs from 10 MMFs with 4-ASK signal transmission are presented in Fig. 10. In Fig. 10(a), the data rate is 300 Mbps. As $P_{r,optical,req}$ increases, the obtained BERs decrease. Furthermore, as $P_{r,optical,req}$ increases to greater than −16 dBm, all BERs become lower than 10^{-10}. It should be noted that one BER curve from Fiber 10

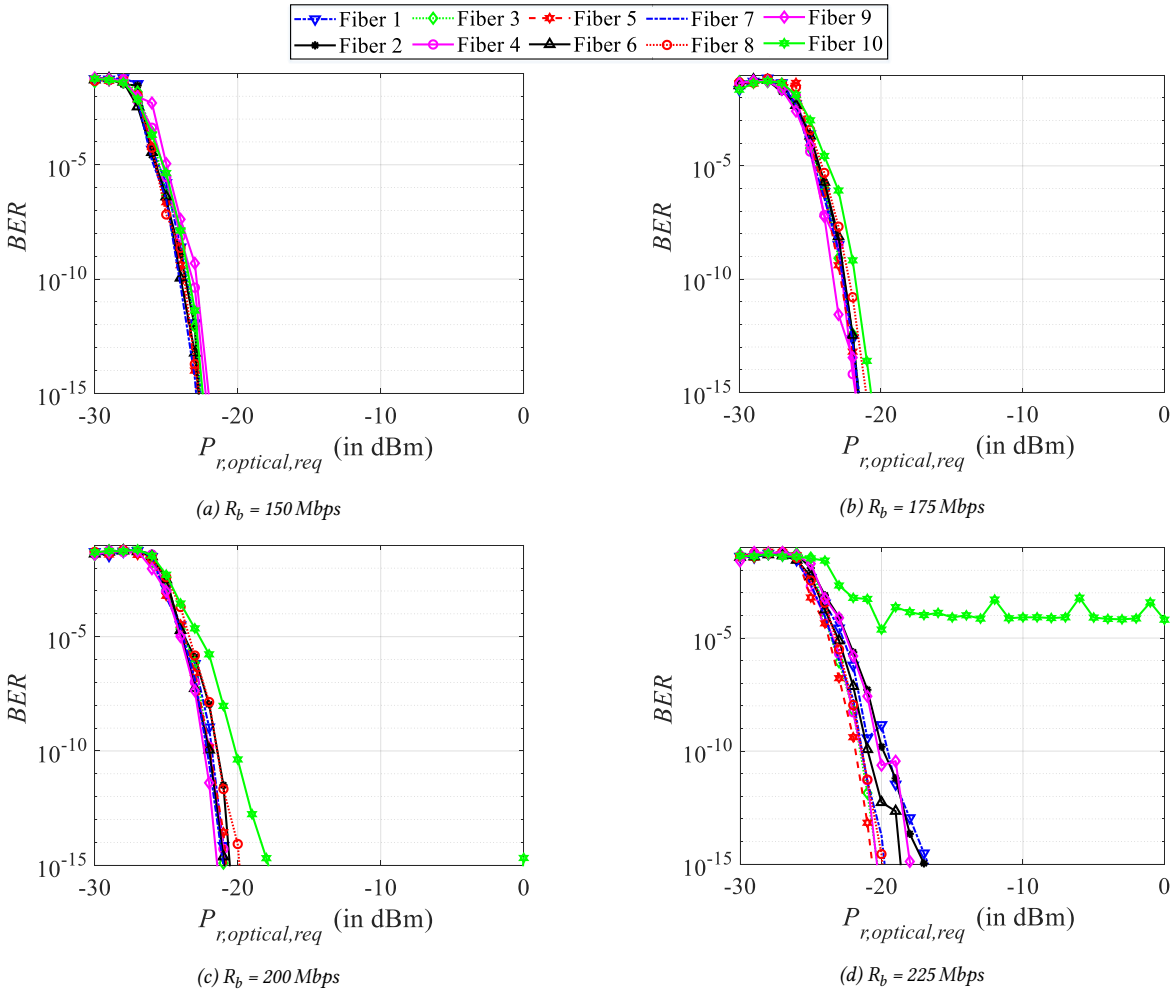

***Fig. 9**: BERs from the OOK signal transmission over the 3-dB modal band (or passband #0).*

fluctuates but is still below 10^{-11} as $P_{r,optical,req}$ increases further. Considering Figs. 10(b), (c), and (d), the data rates used are 350, 400, and 450 Mbps, respectively. The obtained BERs from these three figures are quite poor. As $P_{r,optical,req}$ increases, the BERs can be observed to decrease and become relatively flat at different values. Fig. 10(b) indicates that Fiber 10 has the worst BER of approximately 10^{-6}. Fig. 10(c) shows a similar result in that the worst BER of approximately 10^{-2} was from Fibers 9 and 10. According to Fig. 10(d), where the data rate was increased to 450 Mbps, it can be clearly observed from all 10 MMFs that the obtained BERs were higher than 10^{-6}, with most higher than 10^{-4}. Fig. 10 indicates that the maximum data rate of the 4-ASK signal used with the 3-dB modal band of MMFs was 300 Mbps, 100 Mbps greater than the maximum data rate obtained from OOK. By applying 4-ASK modulation to the 3-dB modal band of MMFs the data rate transmitted over the band showed a comparatively greater increase than that obtained from OOK modulation (which is 200 Mpbs). However, the obtained data rate from 4-ASK modulation was not twice the data rate obtained from OOK since, for 4-ASK, four levels of amplitude needed to be separated at the receiving end. This subsequently led to a high BER when retaining the data rate at twice that obtained from OOK. Thus, the obtained data rate from 4-ASK modulation was lower than expected; that is, 300 Mbps. The data rate for 4-ASK modulation with the 3-dB modal band was used in this study for transmission in passband #0, while other passbands were used for additional data transmission over MMFs.

4.2 Applying DSSS to Passband #2, #3, and #4

As mentioned earlier in Section 2.1, seven passbands (passbands #0 to #6) can be used as channels for signal transmission. However, according to [7], passbands #2 to #4 have been found to be unsuitable for use as sub-channels for SCM transmission due to the uncertainty of their peak frequencies. Rather than leaving these passbands unused, the DSSS was applied here to increase the total data rate. In this section, the performance of the BER in the MMF communication system with SCM and DSSS is studied. There are five different sub-channels including the 3-dB modal band (or passband #0), passband #1, DSSS (covering passbands #2 to #4), #5, and #6. The total data rate of 700 Mbps

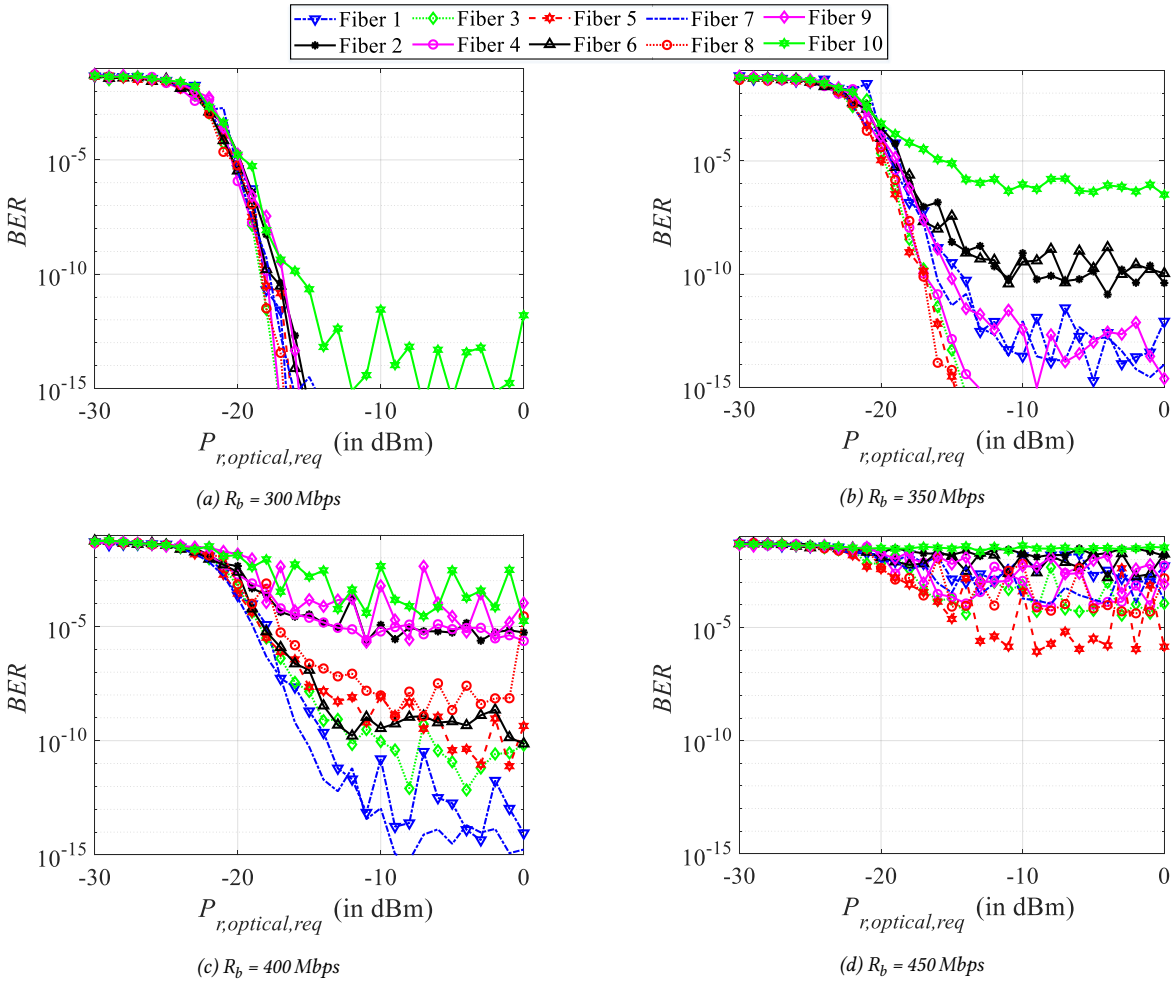

***Fig. 10**: BERs from the 4-ASK signal transmission over the 3-dB modal band (or passband #0).*

is transmitted over an MMF measuring 1 km in length. This data rate is divided into five parts: 300 Mbps for passband #0 with 4-ASK signaling and 100 Mbps each for the other four low-frequency passbands using OOK. The performance of BER in this communication system from 10 different MMFs is shown in Fig. 11.

Fig. 11 shows the BER curves from 10 different MMFs. It can be observed that as $P_{r,optical,req}$ increases, the BERs decrease. Once $P_{r,optical,req}$ is greater than -7 dBm, the BERs become relatively stable reaching the error floor at particular levels depending on the fiber used. For example, for Fiber 8, since $P_{r,optical,req}$ is greater than -9 dBm, the obtained BER is stable at approximately 10^{-14}. As indicated in Fig. 11, most BER curves are below 10^{-9} except those from Fibers 2 and 6. Fiber 6 has the worst BER curve, at which the highest error floor is obtained with a BER of 10^{-7}. Averaging all 10 BER curves, at $P_{r,optical,req}$ greater than -7 dBm, the average BER is 10^{-8}, which is too high for use in practice.

As can be observed, the average BER is mainly affected by the BER from Fiber 6. Hence, to better understand the frequency response of Fiber 6, the subcarrier signals considered are shown in Fig. 12.

Fig. 12 shows the five frequency subcarrier signals located at five different sub-channels: passbands #0, #1, DSSS, #5, and #6. The main frequency components of all subcarrier signals are located at 0, 300, 800, 1311, and 1572 MHz, respectively. As can be observed, the main frequency components of passbands #0 and #1 are located at the peak of the fiber response. The DSSS passband (covering passbands #2 to #4) with a code length of 3 is applied. The subcarrier signal with a data rate of 100 Mbps is then spread out in the frequency domain, covering a bandwidth of 600 MHz. Although transmitting at the same data rate, the frequency components of the DSSS signal are lower than those from the other three subcarrier signals (that is, from passbands #1, #5, and #6). As mentioned earlier, passbands #2 to #4 are not suitable to be used separately as sub-channels. Hence, using the DSSS technique to cover these passbands should increase the tolerance to the frequency-selective nature of these passbands.

When considering the subcarrier signal located at 1311 MHz (passband #5), the main frequency of the subcarrier is observed to be in the vicinity of the null MMF. This should result in a poor received signal for this subcarrier, affecting the whole transmission performance. Similarly, for passband #6, where the main

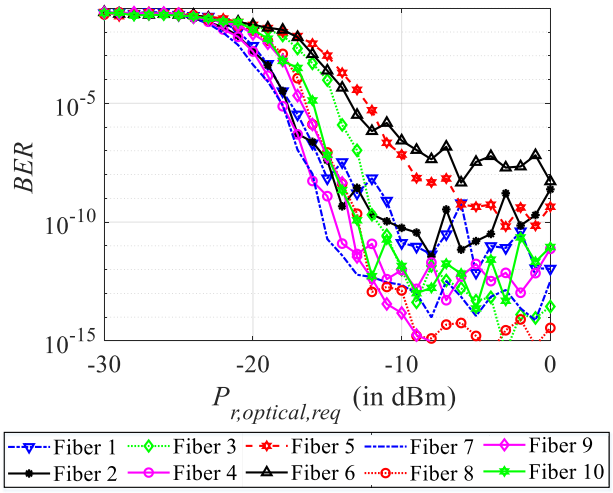

***Fig. 11**: The 10 BER curves with a data rate of 700 Mbps when applying the DSSS technique to passbands #2 to #4.*

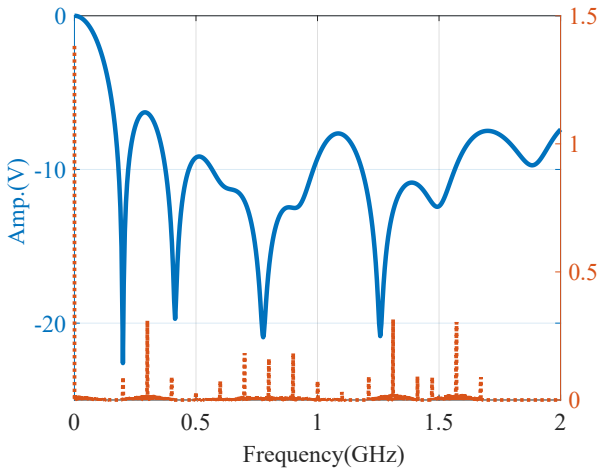

***Fig. 12**: The frequency response of Fiber 6 with the subcarrier frequency components.*

frequency is located at 1572 MHz, the sideband of the subcarrier signal is at the null of the MMF, potentially degrading the received signal.

To better understand the effects of the MMF frequency response to subcarrier signals, eye diagrams of all received subcarrier signals are shown in Fig. 13.

The eye diagrams of the received subcarrier signals from passbands #0, #1, DSSS, #5, and #6 are shown in Figs. 13(a), (b), (c), (d), and (e), respectively. According to Fig. 13(a), there are four different levels of the received signal from passband #0 at which 4-ASK modulation is applied. The eye opening for this received signal is large and clear. At the receiving end, the signal can then be interpreted correctly into bits. Figs. 13(b), (c), (d), and (e) show two different levels of the received signal because OOK modulation is applied to these subcarrier signals. It can be observed from Figs. 13(b), (c), and (e) that the eye opening is large, resulting in the received signals being easily differentiated into bits 0 and 1. It should be noted that for passband #6, the null of the MMF does not strongly affect the subcarrier signal since it is not a deep null, as can be observed from Fig. 12. However, in Fig. 13(d), the eye diagram of the received subcarrier signal from passband #5 is shown to fluctuate strongly at both levels. The eye opening is small and almost closed. This is likely to affect the signal transmission decision process of this passband. To view the performance of each passband, the BERs obtained from different passbands of Fiber 6 are presented in Fig. 14.

Fig. 14 shows all five BER curves for the five received subcarrier signals of Fiber 6. It can be observed that none of the five BER curves monotonically decrease as the received optical power increases but become stable at certain levels. The BER curves for the received subcarrier signals from passbands #0 and #1 are lower than 10^{-9}. Whereas, for the subcarrier signals from the DSSS and #6 passbands, the BER curves vary in the same range between 10^{-11} and 10^{-8}. This result confirms that the use of the DSSS technique in signal transmission over the DSSS passband lessens the effect of the frequency-selective fading channel. On the other hand, the obtained BER curve from passband #5 is the highest of all passbands. The BER floor of this passband signal is higher than 10^{-8}. This result agrees with the previous analysis on the effect of some parts of the frequency component being located near or at the deep null of the MMF frequency response, as shown in Fig. 12 and the eye diagram of this subcarrier signal in Fig. 13(d). To improve the BER performance of this optical communication system, passband #5 should not be used as a separate sub-channel but utilized as a part of the DSSS passband signal, as demonstrated by the following results.

4.3 Applying DSSS to Passband #2, #3, #4, and #5

In this section, four different sub-channels are used in signal transmission: passbands #0, #1, DSSS, and #6. The DSSS covers passbands #2 to #5. This passband then covers a frequency bandwidth of 800 MHz. The data rate transmitted over passbands #0, #1, and #6 is identical to the previous study, namely 300, 100, and 100 Mbps, respectively. However, the data rate for the DSSS passband is changed since it covers a larger bandwidth. The effect of applying the DSSS technique to passbands #2 to #5 is examined in this study.

4.3.1 150-Mbps DSSS passband transmission

In this section, the data rate for the DSSS passband is increased to 150 Mbps, resulting in a total transmission data rate of 650 Mbps. This can be achieved because the DSSS passband now covers a larger bandwidth. To avoid interference between the signals from passbands #1 and DSSS, the subcarrier frequency for the DSSS passband is changed to 900 MHz. The resulting BER curves from 10 different MMFs are shown in Fig. 15.

As can be observed from Fig. 15, when the received

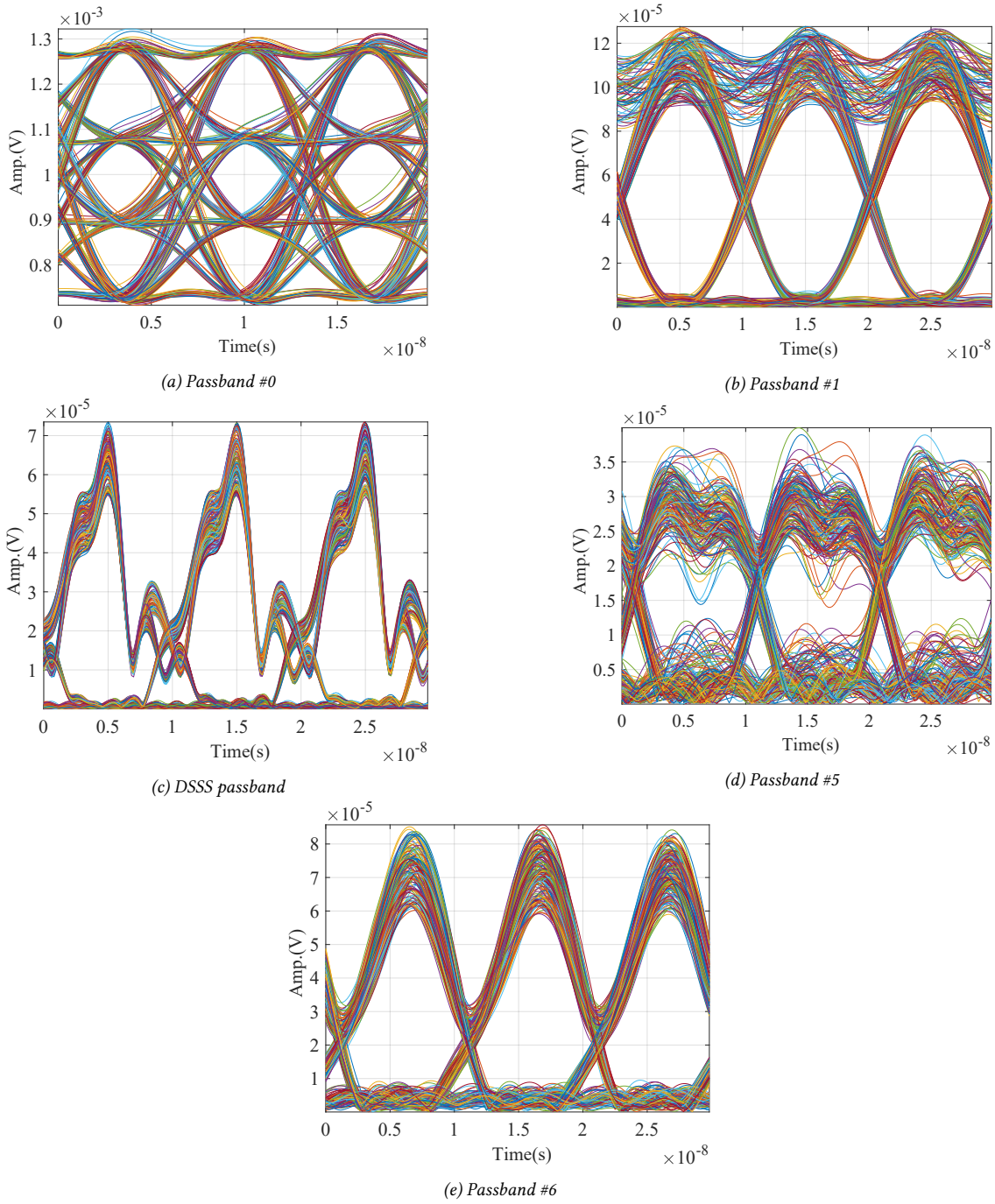

***Fig. 13**: Eye diagrams of the received subcarrier signals from Fiber 6.*

optical power ($P_{r,optical,req}$) is higher than −10 dBm, all BER curves reach the BER floors with a minimum level of 10^{-8}. The highest BER curve is still from Fiber 6. When comparing Figs. 11 and 15, it can clearly be observed that all 10 BER curves in Fig. 15 are higher than those from Fig. 11. Hence, including passband #5 to the DSSS passband and increasing the data rate of the subcarrier signal transmitted over the DSSS passband from 100 Mbps to 150 Mbps does not improve the obtained BER. To better understand the results, the worst BER curve from Fiber 6 is considered. Again, the frequency response of Fiber 6 and subcarrier signals are shown in Fig. 16.

The four subcarrier signals in Fig. 16 are shown in the frequency domain. The subcarrier frequencies of these signals are located at 0, 300, 900, and 1572 MHz, respectively. As can be clearly observed from Fig. 16, the subcarrier signals from passbands #0, #1, and #6 are not at any deep nulls of the MMF. This is unlikely to lead to any poorly received signals from these passbands. However, considering the DSSS passband subcarrier signal with the main subcarrier frequency located at

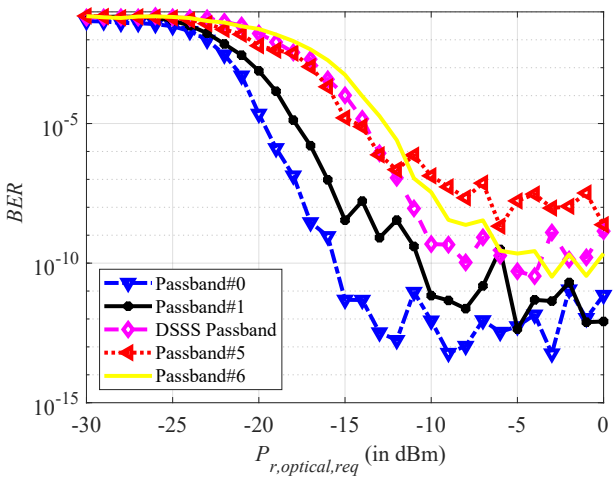

***Fig. 14**: BER curves for each received subcarrier signal from Fiber 6.*

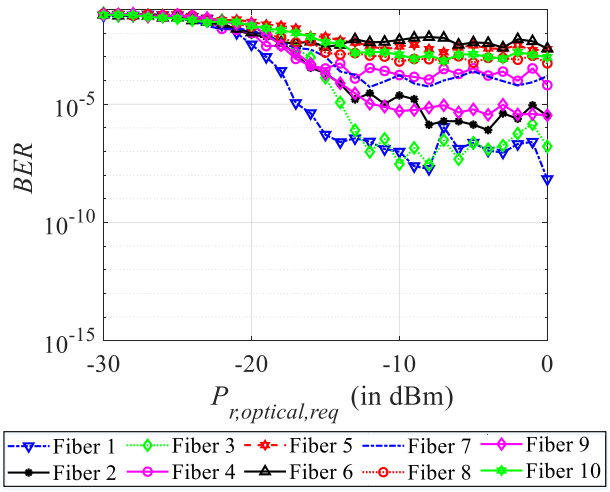

***Fig. 15**: The 10 BER curves with a total data rate of 650 Mbps: DSSS technique with a 150-Mbps data rate covering passbands #2 to #5.*

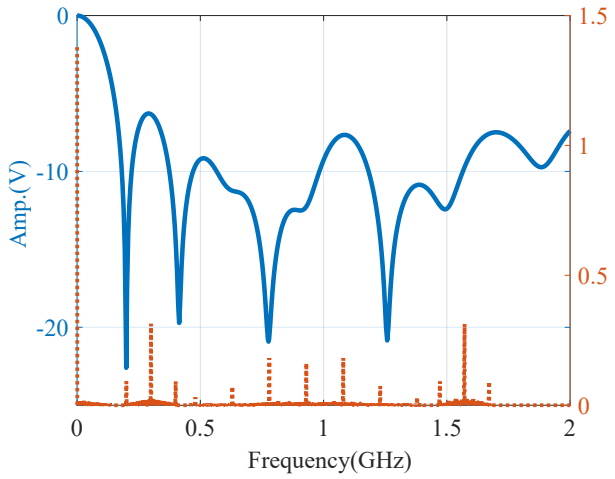

***Fig. 16**: The frequency response of Fiber 6 and the subcarrier frequency components: DSSS technique with a 150-Mbps data rate covering passbands #2 to #5.*

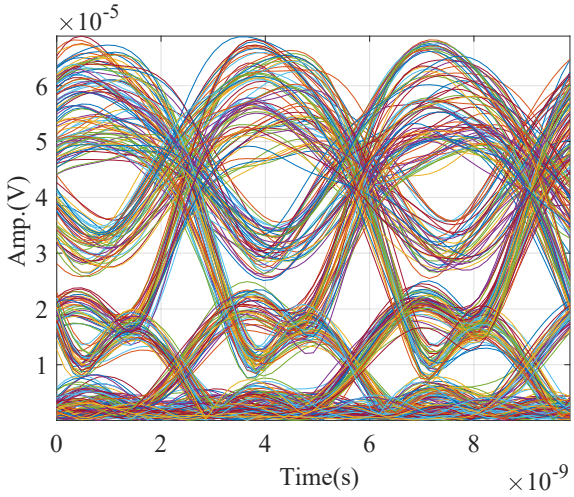

***Fig. 17**: Eye diagram of the received DSSS passband subcarrier signal from Fiber 6: DSSS technique with a 150-Mbps data rate covering passbands #2 to #5.*

900 MHz, the transmission bandwidth is spread out and covers a bandwidth of 900 MHz, which is 1.5 times larger than the DSSS signal transmission bandwidth shown in Fig. 12. This means that the subcarrier signal for the DSSS passband in Fig. 16 will be affected by many nulls from the MMF. As a result, the received signal from the DSSS passband will be much poorer compared to the one presented in Fig. 12. To confirm this analysis, an eye diagram of the DSSS passband received signal from Fiber 6 is shown in Fig. 17.

The eye diagram of the received DSSS passband signal presented in Fig. 17 is very poor, making it very difficult to distinguish between the signals representing bits 0 and 1. This is likely to lead to a very high BER for this subcarrier signal. It can be observed from Fig. 17 that the DSSS technique with a 150-Mbps data rate cannot deliver a good signal. However, this is only from Fiber 6. Fig. 18 shows the performance of different passband signals and the average BERs for different passbands (that is, passbands #0, #1, and DSSS (covering passbands #2 to #5), and #6) from 10 different MMFs.

According to Fig. 18, all average BERs have a floor level lower than 10^{-8} except the average BER from the DSSS passband, where the BER floor is very high at the level of 10^{-3}. This high average BER floor for the DSSS passband confirms the previous analysis concerning the insufficient tolerance when applying the DSSS technique, with a data rate of 150 Mbps, to passbands #2 to #5. Increasing the data rate of the DSSS signal transmission and retaining the same code length of the spreading sequence provides a greater opportunity for the transmitted signal to be degraded by many deep nulls, resulting in a very high obtained BER. However, in this setting, increasing the code length from 3 to 7 is not an

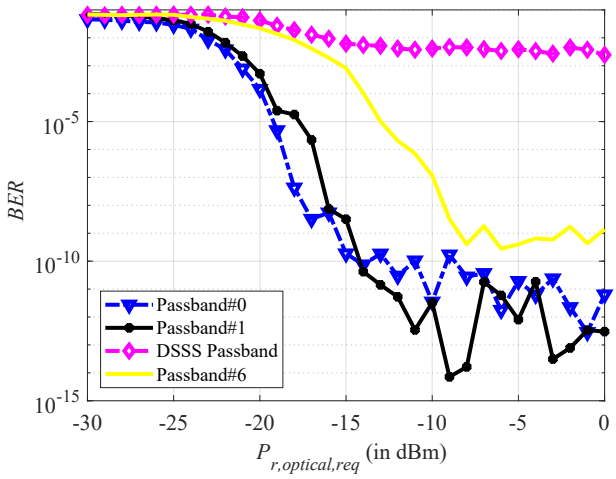

***Fig. 18**: Average BERs from 10 different MMFs: for four different passband signals.*

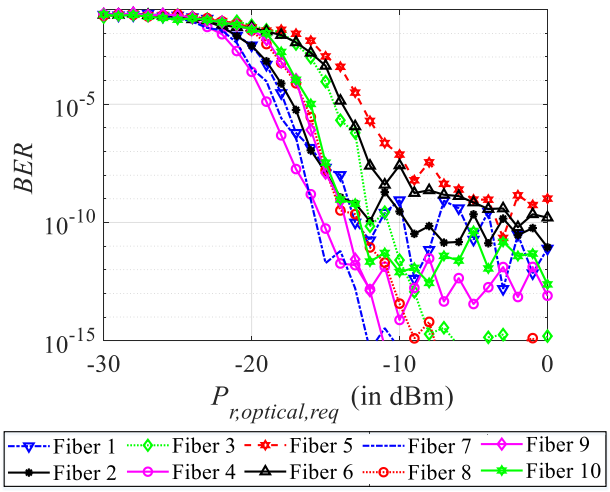

***Fig. 19**: BERs with a total data rate of 600 Mbps: DSSS technique with a 100-Mbps data rate covering passbands #2 to #5.*

option since the required bandwidth will be significantly increased and interfere with the neighboring passband signals. As can be observed, to retain the DSSS passband signal to tolerate the frequency-selective nature of the low-frequency MMF passbands, the data rate transmitted over the DSSS passband must be reduced. In the next section, the data rate of 100 Mbps is used for the DSSS passband, with the total transmission data rate reduced to 600 Mbps.

4.3.2 100-Mbps DSSS passband transmission

As previously mentioned, the total transmission data rate of 600 Mbps is used in this section. This data rate is divided into four parts: 300 Mbps for passband #0, and 100 Mbps each for passbands #1, DSSS (covering passbands #2 to #5), and #6. The performance of BER in this communication system with 10 different MMFs is shown in Fig. 19. It should be noted that the data rate used in the DSSS passband is reduced to 100 Mbps.

From Fig. 19, it can be observed that 10 different BER curves correspond to 10 different MMFs. As the received optical power ($P_{r,optical,req}$) increases, all BERs decrease and reach the BER floors at different levels. It is clear that for all 10 MMFs, the obtained BERs are lower than 10^{-9} since the received optical power is higher than -5 dBm. The BER performance shown in Fig. 19 is significantly improved when compared to that presented in Fig. 11. The improvement is achieved by not using passband #5 as a separate subcarrier channel. Comparing the BERs from Fig. 19 to those in Fig. 15, the BERs from Fig. 19 are observed to be much lower. This improvement is due to the reduction in the data rate transmitted over the DSSS passband, allowing the DSSS modulated signal to be more tolerant to the frequency-selective effects of the passbands.

According to Fig. 19, the DSSS technique is suitable for applying to passbands #2 to #5, using a data rate of 100 Mbps. The total data rate of the SCM MMF communication system is 600 Mbps. However, for Fig. 19,

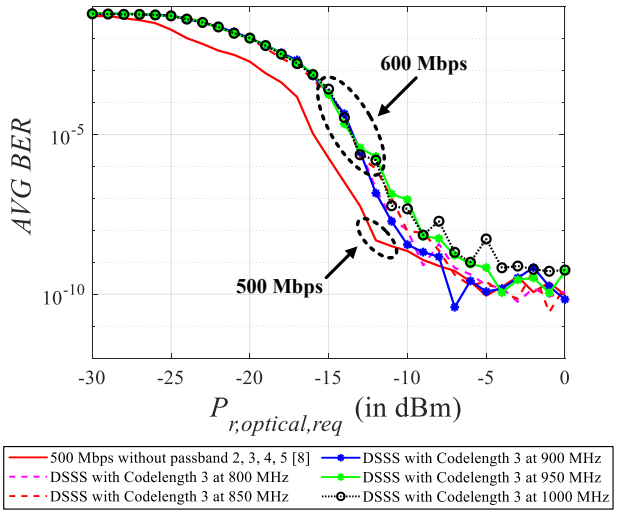

***Fig. 20**: Average BERs of the SCM MMF system using low-frequency passbands: with DSSS at different subcarrier frequencies.*

the center frequency of the DSSS passband signal is located at 900 MHz. It is interesting to determine whether the whole system performance of the obtained BER alters if the center frequency of the DSSS passband signal is changed. This will show the robustness of applying the DSSS technique to the system. The center frequency of the DSSS passband is changed from 900 MHz to 800, 850, 950, and 1000 MHz, respectively. The average system BER from 10 different MMFs is determined for each case, as shown in Fig. 20.

The BER performance of the SCM MMF system using low-frequency passbands with the DSSS technique is presented in Fig. 20. The code length used for the DSSS is 3. To determine the robustness of the system, the center frequencies for use with the DSSS passband are varied to 800, 850, 900, 950, and 1000 MHz. The data rate

transmitted over this DSSS passband is 100 Mbps, and the total system data rate is 600 Mbps. Fig. 20 indicates that the average BERs obtained from five different DSSS cases are almost identical to each other. As the received optical power increases, the obtained BER decreases and reaches the BER floor at a maximum BER of 10^{-9} (as indicated by the black dotted line with circular markers), which is suitable for use in practice. Furthermore, as the center frequency of the DSSS passband is varied among five different frequencies (that is, 800, 850, 900, 950, and 1000 MHz), the whole BER system remains approximately the same. This demonstrates the robustness of the system with the DSSS technique for use with low-frequency MMF passbands. These five BER curves from the DSSS technique are also compared to the BER curve obtained when the DSSS is not applied to passbands #2 to #5 [8]. The obtained BERs from these two cases reach the BER floor of 10^{-9} at the received optical power greater than −5 dBm. However, with DSSS technique applied, the total data rate is 600 Mbps, which is 100 Mbps higher than without the DSSS technique. It can be observed that rather than leaving passbands #2 to #5 unused due to uncertainty in the suitable peak frequencies of the passbands being used, applying the DSSS technique to these passbands can help increase the system data rate while keeping the whole system performance for BER below 10^{-9}.

With this proposed system, the possible data rate of MMFs, especially over a short distance (for example, in a building), can be increased two or three-fold compared to the conventional system. This means that with a high data transmission current requirement, the existing MMFs can be used effectively.

5. CONCLUSION

The performance of signal transmission over a 1-km MMF using SCM and DSSS techniques was analyzed in this study. The DSSS technique was adopted over a DSSS passband, covering low-frequency passbands #2 to #5 to reduce the effect of a frequency-selective fading channel. The 3-dB modal band and the other three low-frequency passbands of an MMF were adopted as channels for transmitting subcarrier signals. The 4-ASK modulation was applied over the 3-dB modal band. For the other three low-frequency passbands: #1, DSSS, and #6, the subcarrier signals were OOK-modulated. The findings of this study reveal that the DSSS is a promising technique for use with low-frequency MMF passbands. The system was found to be robust for varying the center frequency of the DSSS signal. A system BER lower than 10^{-9} with a total data rate of 600 Mbps was obtained without applying any error-correction codes. The proposed DSSS technique can therefore be utilized efficiently with all low-frequency MMF passbands, leaving none unused.

ACKNOWLEDGMENTS

This work was supported by Naresuan University, Thailand.

REFERENCES

[1] A. Rahim *et al.*, "16-channel O-OFDM demultiplexer in silicon photonics," in *Optical Fiber Communication Conference*, 2014.

[2] C.-T. Tsai *et al.*, "Multi-mode VCSEL chip with high-indium-density InGaAs/AlGaAs quantum-well pairs for QAM-OFDM in multi-mode fiber," *IEEE Journal of Quantum Electronics*, vol. 53, no. 4, pp. 1–8, Aug. 2017.

[3] K. Nagashima, T. Kise, Y. Ishikawa, and H. Nasu, "A record 1-km MMF NRZ 25.78-Gb/s error-free link using a 1060-nm DIC VCSEL," *IEEE Photonics Technology Letters*, vol. 28, no. 4, pp. 418–420, Feb. 2016.

[4] K. Benyahya *et al.*, "High-speed bi-directional transmission over multimode fiber link in IM/DD systems," *Journal of Lightwave Technology*, vol. 36, no. 18, pp. 4174–4180, Sep. 2018.

[5] J. Patmanee and S. Kanprachar, "Analysis of the multimode fiber at low-frequency passband region," *Journal of Telecommunication, Electronic and Computer Engineering*, vol. 9, no. 2-6, pp. 37–41, 2017.

[6] J. Patmanee, C. Pinthong, and S. Kanprachar, "Performance of subcarrier multiplexing transmission over multimode fiber at low-frequency passbands," in *2017 8th International Conference of Information and Communication Technology for Embedded Systems (IC-ICTES)*, 2017, pp. 160–164.

[7] S. Kanprachar, C. Pinthong, and J. Patmanee, "BER performance of multimode fiber low-frequency passbands in subcarrier multiplexing transmission," in *Third International Conference on Photonics Solutions (ICPS2017)*, 2018.

[8] J. Patmanee and S. Kanprachar, "Performance of signal transmission via subcarrier multiplexing with 4-ASK over low-frequency passbands of multimode fibers," in *2019 58th Annual Conference of the Society of Instrument and Control Engineers of Japan (SICE)*, Hiroshima, Japan, 2019, pp. 623–628.

[9] X. Zuo, D. Wang, and R. Yao, "On performance of MRC-FDE UWB system with direct sequence spreading," in *2013 IEEE International Conference on Signal Processing, Communication and Computing (ICSPCC 2013)*, 2013.

[10] Y. R. Zheng, Z. Yang, M. Yue, B. Han, Z. Chen, and J. Wang, "DSP implementation of direct-sequence spread spectrum underwater acoustic modems with networking capability," in *2014 Oceans - St. John's*, 2014.

[11] S. Wang, J. An, Y. Ren, T. Wang, and X. Bu, "Compressed receiver for multipath DSSS signals," *IEEE Communications Letters*, vol. 18, no. 8, pp. 1359–1362, Aug. 2014.

[12] A. Pottier, F.-X. Socheleau, and C. Laot, "Quality-of-service satisfaction games for noncooperative underwater acoustic communications," *IEEE Access*, vol. 6, pp. 21 467–21 481, 2018.

[13] J. Harshan and Y.-C. Hu, "Cognitive radio from

hell: Flipping attack on direct-sequence spread spectrum," in *2018 IEEE Wireless Communications and Networking Conference (WCNC)*, 2018.

[14] P. I. Puzyrev, V. Y. Shein, and V. V. Erohin, "Orthogonal multiple chirp modulation for tasks of robust data transmission," in *2018 19th International Conference of Young Specialists on Micro/Nanotechnologies and Electron Devices (EDM)*, 2018, pp. 6403–6408.

[15] L. W. Couch, *Digital and Analog Communication Systems*, 8th ed. New York, USA: Pearson, 2013, pp. 358–360.

[16] R. E. Ziemer and W. H. Tranter, *Principles of Communications: Systems, Modulation, and Noise*, 7th ed. New York, USA: John Wiley & Sons, 2014, pp. 528–536.

[17] A. Goldsmith, *Wireless Communications*. Cambridge, UK: Cambridge University Press, 2005, pp. 409–419.

[18] W. Stallings, *Data and Computer Communications*, 10th ed. New York, USA: Pearson, 2013, p. 179.

[19] G. Keiser, *Optical Fiber Communications*, 5th ed. Singapore: McGraw-Hill Education, 2015, pp. 285–286.

[20] M. Velichko and O. Nanii, "Increase of transmission speed in access networks using 4-ary ASK directly modulated lasers," in *2006 International Workshop on Laser and Fiber-Optical Networks Modeling*, 2006, pp. 202–205.

Jaruwat Patmanee received his B.S. degree and M.S. degree in electrical engineering from Naresuan University, Phitsanulok, Thailand, in 2014 and 2017, respectively. Currently, he is a Ph.D. student in electrical engineering at Naresuan University, Phitsanulok, Thailand. His research interests are mainly focused on optical communication system and coding theory.

Surachet Kanprachar received his B.Eng. degree (first-class honors) in Electrical Engineering in 1996 from Chulalongkorn University, Bangkok, Thailand. He received both the M.Sc. and Ph.D. degrees in Electrical Engineering from the Virginia Polytechnic Institute and State University (VA Tech), Blacksburg, Virginia, USA in 1999 and 2003, respectively. Since 2003, he has been with the Department of Electrical and Computer Engineering, Faculty of Engineering, Naresuan University, Phitsanulok, Thailand, where he is now an associate professor. His research interests are in the area of optical fiber communications, coding theory, and artificial intelligence.